Simple Optical Models for Diagnosing Surface-Atmosphere Shortwave Interactions

Michael Winton

Geophysical Fluid Dynamics Laboratory/NOAA

Revised for *Journal of Climate*

11 February 2005

Corresponding author: Dr. Michael Winton, GFDL/NOAA, P.O. Box 308, Princeton University Forrestal Campus, Princeton, NJ 08542. email: Michael.Winton@noaa.gov, phone: (609) 452-6531, FAX: (609) 987-5063

Abstract

A technique is developed for diagnosing effective surface and atmospheric optical properties from climate model shortwave flux diagnostics. These properties can be used to distinguish the contributions of surface and atmospheric optical property changes to shortwave flux changes at the surface and top of the atmosphere and also to predict the shortwave response to optical property changes. In addition to standard shortwave flux diagnostics, the technique makes use of two diagnostics obtained from an auxiliary shortwave calculation over a perfectly absorbing (zero albedo) surface. The technique is tested using auxilliary shortwave calculations and shown to predict the monthly mean surface absorption at four validation albedos with an RMS error less than 2% over the globe. The reasons for the accuracy of the technique are explored. Less accurate techniques that make use of existing shortwave diagnostics are presented and compared.

I. Introduction

The absorption and reflection of shortwave radiation by the earth's atmosphere and surface serve as fundamental drivers of the climate system. Kiehl and Trenberth (1997) review estimates of the earth's shortwave budget. Of the 342 W/m^2 incident at the top of the atmosphere (TOA), they estimate that 31% is reflected, 20% is absorbed in the atmosphere, and 49% is absorbed at the surface. They estimate the planetary and surface albedos at 31% and 15% respectively. Because so much of the earth's surface is ice-free ocean with a very low reflectivity, the most important atmosphere-surface shortwave interaction is the *shielding* effect of clouds that prevents surface absorption. The cloud shielding effect is diagnosed using the cloud shortwave forcing -- the difference in shortwave absorption between actual conditions and a hypothetical clear (cloudless) sky. Globally, the cloud shortwave forcing is 14% of the TOA downward shortwave (Harrison et al 1993). It is largest over the ocean in the subpolar and tropical warm pool regions. The concept of cloud shortwave forcing depends upon the availability of a fixed reference surface albedo. Cloud shortwave forcing will change when the surface albedo changes even with no change in cloudiness.

Over a reflective surface, the change in absorption due to altered cloudiness is influenced by the surface albedo through multiple cloud-ground reflections. Observational studies in polar regions have noted that the downward shortwave at the surface is considerably larger, sometimes nearly a factor of two larger, over bright ice surfaces than over dark ocean surfaces for similar atmospheric conditions (Rouse 1987, Freese and Kottmeier 1998, and Wendler et al 2004). Fig. 1 shows the fraction of the annual surface downward shortwave that is due to multiple reflection in the GFDL AM2 global atmosphere/land model (GFDL GAMDT 2004). This is determined by instrumenting the model to make an extra shortwave calculation with a surface albedo of zero (perfectly absorbing) replacing the mdel-calculated surface albedo. The difference between the model-calculated-albedo downward and the zero-surface-

albedo downward fluxes is the multiply reflected portion. Figure 1 shows that the largest values are over the polar sea ice where, typically, 10-20% of the annual mean downward shortwave has been multiply reflected. There is also a significant multiply reflected fraction over the high latitude continents. In spite of presenting the most reflective surface, the ice sheets have less multiple reflection than the sea ice regions due to the low reflectivity of the overlying air. Multiple reflections serve to increase surface absorption by increasing the surface downward flux for a given atmospheric transmissivity. During multiple reflection and on the final trajectory of the reflected shortwave toward space there are opportunities for atmospheric absorption. This absorption reduces the impact of surface albedo upon the TOA shortwave budget relative to its impact on the surface budget.

There is particular interest in surface-atmosphere shortwave interaction for those regions of the earth where both surface and atmospheric optical properties respond to climate change. In the Arctic, models with anthropogenic forcing predict and recent observations confirm increases in summer cloud cover accompanying diminished sea ice cover (Comiso 2002; Holland and Bitz 2003; Wang and Key 2003; Vinnikov et al 1999). To resolve the considerable differences in the simulation of future Arctic climate change (Holland and Bitz 2003), it will be useful to distinguish the sources of the differences in the predictions of the Arctic shortwave budget.

To summarize, attributing changes in the shortwave budget to atmospheric and surface changes in ice-covered regions is more difficult than in other regions and requires a more sophisticated analysis technique. The technique must account for three surface-atmospheric shortwave interactions, shown schematically in Figure 2:

1. *Shielding*. The atmosphere shields the surface by reflecting and absorbing a certain fraction of the downward radiation. The shielding effect of the atmosphere is characterized by its transmissivity to downward radiation.

2. *Multiple reflection*. Radiation reaching the surface may undergo several reflections between the clouds and surface before being absorbed or escaping from the surface. The albedo of the surface and of the atmosphere to upward radiation both contribute to multiple reflection.
3. *Atmospheric compensation*. Upward radiation from the surface may be absorbed by the atmosphere before it can escape to space. The absorptivity of the atmosphere to upward radiation is its most important quality for this atmospheric compensation effect.

The goal of this paper is to develop simple models based on Figure 2 that characterize the atmospheric and surface optical properties for the purpose of diagnosing their individual impacts on the surface and atmospheric shortwave absorption. The GFDL AM2 atmosphere/land model (GFDL GAMDT, 2004) has been specially instrumented with extra shortwave calculations to estimate and validate these atmospheric optical parameters. The shortwave calculation in the model follows Freidenreich and Ramaswamy (1999) with modifications to improve performance. These modifications include a reduction in the number of spectral bands treated and the use of an effective angle for diffuse radiation (53^o) rather than a 4-point quadrature scheme. AM2 does not treat the spectral dependence of surface reflection.

In the next section we will introduce a technique that characterizes the averaged shortwave behavior of an atmosphere with four optical parameters. In the following section, three alternative methods that do not require an extra shortwave calculation are presented and compared with the 4-parameter model. The fourth section explores the reasons for the difference in upward and downward reflectivity that is important to the superior accuracy of the 4-parameter model. Results are summarized and discussed in the final section.

II. The 4-parameter model

The 4-parameter model equations

In this model, four bulk optical parameters characterize the atmosphere: upward and downward reflectivities and transmissivities (Fig. 2). These optical properties are related to directional shortwave fluxes at the top and bottom of the atmosphere by the equations:

$$S_{T\uparrow} = \alpha_{\downarrow} S_{T\downarrow} + \tau_{\uparrow} S_{B\uparrow} \quad (1)$$

$$S_{B\downarrow} = \tau_{\downarrow} S_{T\downarrow} + \alpha_{\uparrow} S_{B\uparrow} \quad (2)$$

$$S_{B\uparrow} = \alpha_S S_{B\downarrow} \quad (3)$$

where Table 1 defines the notation. To solve these equations for the five optical parameters we use the in situ surface albedo fluxes that are customarily produced by climate models in combination with additional fluxes calculated over a perfectly absorbing surface. In this case equations 1 and 2 become:

$$S_{T\uparrow}(\alpha_S = 0) = \alpha_{\downarrow} S_{T\downarrow} \quad (4)$$

$$S_{B\downarrow}(\alpha_S = 0) = \tau_{\downarrow} S_{T\downarrow} \quad (5)$$

Equations 1, 2, 4, and 5 can then be solved for the atmospheric optical properties:

$$\alpha_{\downarrow} = S_{T\uparrow}(\alpha_S = 0) / S_{T\uparrow} \quad (6)$$

$$\tau_{\downarrow} = S_{B\downarrow}(\alpha_S = 0) / S_{T\uparrow} \quad (7)$$

$$\alpha_{\uparrow} = \left(S_{B\downarrow} - S_{B\downarrow}(\alpha_S = 0)\right) / S_{B\uparrow} \quad (8)$$

$$\tau_{\uparrow} = \left(S_{T\uparrow} - S_{T\uparrow}(\alpha_S = 0)\right) / S_{B\uparrow} \quad (9)$$

Six diagnostic quantities are needed to solve for the atmospheric and surface optical properties: $S_{T\downarrow}$, $S_{T\uparrow}$, $S_{B\downarrow}$, $S_{B\uparrow}$, $S_{T\uparrow}(\alpha_S = 0)$, and $S_{B\downarrow}(\alpha_S = 0)$. The last two come from an extra shortwave calculation in the model, analogous to the extra radiation calculation with clouds removed commonly used

to generate clear sky fluxes. In the GFDL AM2 model, the extra calculation incurs negligible extra computation expense. This is because the shortwave algorithm is separated into a part that calculates the optical properties of the individual layers using the delta-Eddington approximation and a part that combines the layers, using the adding method. The surface albedo is only involved in the second part, which is considerably less computationally intensive than the first. This is in contrast to the situation for the clear-sky diagnostics that require both parts of the algorithm. The overall runtime of the model was increased by less than 1% due to the extra computation needed for the zero surface albedo fluxes.

Optical properties can be formed to represent the spatial-temporal average behavior of the atmosphere by using appropriately averaged fluxes on the right hand sides of equations 6--9. In general, these *effective* optical properties will be different from, and more useful than, the similarly averaged optical properties. A familiar example of this is the effective surface albedo formed as the ratio of the time-averaged upward surface shortwave to the time-averaged downward surface shortwave. This quantity is more useful than the time-averaged surface albedo which cannot be multiplied by the time-averaged downward shortwave to give the time-averaged upward shortwave. This is because it gives equal weighting to periods when the insolation is low and high. Nighttime albedos contribute significantly to the time average albedo even though they have no impact at all on surface reflection. The effective surface albedo can be shown to be a time average weighted with the downward surface shortwave:

$$\alpha_{eff} = \frac{\int S_{B\uparrow} dt}{\int S_{B\downarrow} dt} = \frac{\int \alpha S_{B\downarrow} dt}{\int S_{B\downarrow} dt} \qquad (10)$$

The ability to form effective optical parameters for a spatial-temporal region is a powerful capability of this scheme and also contributes substantially to its accuracy as will be discussed section four. Care should be exercised in the interpretation of effective parameters because averaging introduces interdependencies between them. For example, the effective surface albedo is dependent upon the

atmospheric parameters that play a role in the downward shortwave at the surface used for weighting: the downward transmissivity and upward reflectivity.

Figure 3 shows the effective optical properties representing the annual mean behavior of the AM2 model climatology. The downward reflectivity is strongly influenced by cloud and shows high values in the subpolar and Arctic oceans and low values in the subtropics. The correlation of monthly downward reflectivity and low cloud amount is 0.85. The upward reflectivity has a similar pattern but lower values in the subpolar and Arctic oceans. Its monthly correlation with low cloud is only 0.64. The reasons for the differences in upward and downward reflectivities will be discussed in section four. The upward and downward absorptivities are even more different from each other. The downward absorptivity is considerably larger and has an interhemispheric gradient. The upward absorptivity is more symmetric around the equator. Neither of the absorptivities is particularly well correlated with cloud variables. The clear sky counterparts to the Fig. 3 optical properties have also been calculated (not shown). These have higher values over Europe and eastern North America, presumably due to the presence of aerosols. For both reflectivities and the downward absorptivity, the clear sky values are much smaller, but the clear and all sky upward absorptivities have similar magnitudes.

An important application of the bulk optical properties is to predict changes in atmospheric and surface shortwave absorption. From equations 1--3 we can derive expressions for the planetary albedo (α_P), the atmospheric absorption ratio (A_A), and the surface absorption ratio (A_S). The absorption ratios are the atmospheric and surface absorptions divided by the top of atmosphere downward flux, so the three quantities sum to one:

$$\alpha_P = \alpha_\downarrow + \tau_\downarrow \tau_\uparrow \alpha_S / \left(1 - \alpha_S \alpha_\uparrow\right) \tag{11}$$

$$A_A = 1 - \alpha_\downarrow - \tau_\downarrow \left(1 - \alpha_S \left(1 - \tau_\uparrow\right)\right) / \left(1 - \alpha_S \alpha_\uparrow\right) \tag{12}$$

$$A_S = \tau_\downarrow \left(1 - \alpha_S\right) / \left(1 - \alpha_S \alpha_\uparrow\right) \tag{13}$$

In Figure 4, these quantities are plotted as a function of surface albedo for atmospheric parameter values representing the annual mean Arctic atmosphere in AM2. The values at the left edge of the plot define the downward atmospheric parameters. At zero surface albedo, the surface absorbs all of and only the downward transmitted light (there are no multiple reflections) so the downward transmissivity is equal to the zero-surface-albedo surface absorption ratio. Likewise the planetary albedo is equal to the atmospheric downward reflectivity since there are no surface reflections. And, finally, the atmosphere absorbs only downward shortwave so the atmospheric absorption ratio is equal to the downward absorptivity. Figure 4 shows that as the surface albedo increases the surface absorption ratio decreases becoming zero when the surface is perfectly reflective. There is a slight curvature to the absorption due to multiple reflection. Equation 13 shows that if the upward reflectivity were zero the dependence of surface absorption upon surface albedo would be linear – a straight line between the atmospheric transmissivity at zero surface albedo and zero at a surface albedo of one. The effect of multiple reflection is to increase surface absorption by the amount that the surface absorption ratio bows above this straight line.

Careful examination of Figure 4 shows that the atmospheric absorption ratio increases slightly as surface albedo increases. This is due to the atmospheric compensation effect discussed above. We can quantify this effect by differentiating Equations 11 and 13 and forming the ratio of the surface albedo sensitivities of planetary absorption (A_P=1-α_P) and surface absorption:

$$\frac{\partial A_P}{\partial \alpha_S} / \frac{\partial A_S}{\partial \alpha_S} = 1 - \frac{\varepsilon_\uparrow}{1-\alpha_\uparrow} \qquad (14)$$

where $\varepsilon_\uparrow \equiv 1-\alpha_\uparrow-\tau_\uparrow$ (see Table 1). The ratio is less than one because of atmospheric absorption of upward reflected shortwave. The decrement from one is plotted in Figure 5. The pattern is controlled by the pattern of upward absorptivity (Fig. 3). The monthly atmospheric compensation and upward absorptivity have a correlation of 0.9. The values are generally small, ranging from about 12% broadly

over the tropics to 6% and less in high latitudes. The smallness of the values indicates that a first order understanding of the impact of surface albedo can be obtained by focusing on its effect on the surface shortwave budget, bearing in mind that the TOA surface albedo sensitivity will be slightly less.

III. Accuracy of the 4-parameter model and three alternative models

The accuracy of the 4-parameter model is assessed by comparing its prediction of surface and atmospheric absorption ratios (Equations 12 and 13) with computed values at four validation surface albedos: 0.2, 0.4, 0.6, and 0.8. Extra calls to the model's shortwave calculation using these four surface albedos are made to compute the true absorption ratio. Figure 6 plots the computed and estimated values of the monthly mean absorptions at these albedos for the entire year over the entire globe (only every 9^{th} model grid point is plotted to keep the figure manageable). There is slight tendency to underestimate surface absorption when it is small but, overall, the accuracy of the technique is very good. The correlations of the estimates with the actual values are over 0.99.

The accuracy of the 4-parameter model argues for the online calculation of the extra diagnostics it requires; the zero-surface-albedo surface and top of atmosphere fluxes. Since, these diagnostics have not yet been implemented in most climate models, we explore the accuracy of three simpler techniques that make use of existing diagnostics. Of the three, only the second provides an estimate of the atmospheric as well as the surface absorption as a function of surface albedo. The estimates of the three techniques along with the 4-parameter estimates and actual calculated absorptions for the Arctic in AM2 are shown in Figure 7. It is noteworthy that the 4-parameter technique makes a small underestimate of surface absorption for high surface albedos, consistent with Fig. 6a but, overall, is very accurate.

The first alternative technique, the *linear* method, gives the surface absorption as a linear function of surface albedo. The line is anchored at two albedos: (1) the in situ albedo, α_{S0}, determined as the ratio of

monthly upward to downward surface shortwave flux and (2) an albedo of one, where the surface absorption is zero. The linear approximation is:

$$A_S = S_{B\downarrow}(\alpha_S = \alpha_{S0})(1-\alpha_S) \tag{15}$$

This technique is often used for "back of the envelope" calculations. The linear approximation for the AM2 Arctic is shown as the black dashed line in Figure 7. The technique generally overestimates the sensitivity of surface absorption to surface albedo. It will be relatively more accurate when the upward reflectivity and in situ albedo are small. The later is true because a greater range of albedos will fall into the right, interpolated, part of the curve, rather than to the left where the scheme extrapolates. The linear technique cannot be used to estimate the TOA sensitivity to surface albedo, but, as noted above, the TOA sensitivity is dominated by the surface sensitivity.

The second alternative to the 4-parameter model is the *2-parameter* model. This model characterizes the atmosphere with a single reflectivity and transmissivity (or absorptivity), neglecting differences between upward and downward properties. The in situ albedo fluxes are then sufficient to solve equations 1--3 for the two parameters:

$$\alpha = \left(S_{T\downarrow}S_{T\uparrow} - S_{B\downarrow}S_{B\uparrow}\right)/\left(S_{T\downarrow}{}^2 - S_{B\uparrow}{}^2\right) \tag{16}$$

$$\tau = \left(S_{T\downarrow}S_{B\downarrow} - S_{T\uparrow}S_{B\uparrow}\right)/\left(S_{T\downarrow}{}^2 - S_{B\uparrow}{}^2\right) \tag{17}$$

These then replace their directional counterparts in equations 11—13. The 2-parameter approximations for the AM2 Arctic are shown as the dashed gray lines in Figure 7. As with the linear scheme, the two-parameter scheme interpolates to higher albedos and extrapolates to lower albedos. The figure shows that the failure to distinguish upward and downward atmospheric properties results in a significant increase in error. The upward reflectivity and absorptivity are considerably smaller than their downward counterparts in the 4-parameter model (Figure 3). The overestimate of upward absorptivity leads to excessive atmospheric compensation – widening of the atmospheric absorption ratio as the albedo

increases. The overestimate of upward reflectivity leads to excessive curvature of the surface absorption curve.

Since the surface absorption is known at two points, the in-situ and perfect reflecting surface albedos, we only need an estimate of the upward atmospheric reflectivity to obtain the curvature and a complete estimate of the surface absorption. A direct way to obtain an upward atmospheric reflectivity for estimating surface absorption is to parameterize it with available diagnostics. For this purpose we use the ratio of the downward surface shortwave to its clear-sky value. An attempt was made to fit this quantity to the 4-parameter upward reflectivity but it was discovered that significantly different fits are obtained using daily and monthly data. The reason for this has to do with averaging and will be discussed in the next section. Lacking a stable fit, a formula was chosen using physical reasoning:

$$\alpha_{\uparrow} = 0.05 + 0.85\left(1 - S_{B\downarrow} / S_{B\downarrow CLR}\right) \qquad (18)$$

This estimate is plotted against the 4-parameter upward reflectivity in Fig. 8 using daily (light marks) and monthly (dark marks) mean data. The estimate is closer to the daily values and, in general, will overestimate the effective monthly upward reflectivity. Equation 18 is not a fit but rather uses round numbers -- recognizing that clear skies have some small reflectivity and an opaque atmosphere has absorption as well as reflection. The use of an all-sky/clear-sky ratio is a common technique for reducing the influence of solar geometry. The estimate of surface absorption based on equation 18 is:

$$A_S = S_{B\downarrow}\left(\alpha_S = \alpha_{S0}\right)\left(1 - \alpha_S\right)\left(1 - \alpha_{\uparrow}\alpha_{S0}\right)/\left(1 - \alpha_{\uparrow}\alpha_S\right) \qquad (19)$$

where α_{S0} is the in situ surface albedo. As shown in Figure 7 this technique, termed *ALL/CLR*, gives a somewhat better estimate of the Arctic surface absorption than the 2-parameter model but, as expected from Fig. 8, slightly overestimates the upward reflectivity.

Figure 9 reports the RMS fractional error in surface absorption at the four validation albedos (0.2, 0.4, 0.6, and 0.8) for all months of the year and for all locations of the globe (gray bars) and in the Arctic

(black bars). The 4-parameter scheme is the most accurate of the four methods. Two factors lead to the superior accuracy of the 4-parameter method: avoidance of extrapolation error and distinction between downward and upward optical properties. Of the three techniques that use existing diagnostics, the ALL/CLR (eqn. 18) is the best, particularly for the Arctic. In spite of the fact that the ALL/CLR technique has not been fit to the model, its RMS error is only 1% or so larger than that of the 4-parameter technique.

IV. Downward and upward atmospheric properties

In this section we look at the reasons for the differences in downward and upward atmospheric optical properties diagnosed with the 4-parameter method. These differences are critical to the superior accuracy of the 4-parameter technique. We might expect downward and upward properties to be different for several reasons:

1. Downward radiation is partly direct and partly diffuse while all of the upward shortwave is diffuse (the surface reflection is Lambertian in AM2). The different geometries of direct and diffuse optical paths lead to differing optical thicknesses of the atmosphere for the upward and downward directed radiation.
2. Atmospheric absorption occurs in specific spectral bands. As the shortwave stream becomes depleted in these bands the remaining radiation becomes less susceptible to absorption. This effect might lead the upward stream to experience relatively more reflection and transmission than the downward.
3. Differences in the vertical distribution of absorption and reflection can result in different properties of the aggregate layer to incident shortwave from above and below. For example, an absorptive layer over a reflective layer will appear more absorptive from above and more reflective from below.

4. Effects of averaging can lead to differences because the downward properties are averaged with weighting by the top of atmosphere downward radiation while upward properties are weighted with upward shortwave from the surface.

Figure 10 shows the difference in the downward and upward reflectivities representing the AM2 annual climatology. The geometric effect (item 1 above) is generally evident in the difference: the atmosphere is less reflective to downward shortwave in the tropics where the direct path is shorter than the diffuse but more reflective in mid- to high-latitudes where the direct path is longer. The relatively larger difference in the reflectivities in cloudy mid-latitude regions is inconsistent with the geometric effect, however. Clouds convert part of the downward shortwave from direct to diffuse and so tend to make the upward and downward paths more similar.

The reduction in upward reflectivity in cloudy area turns out to be due to the different weighting of the upward properties that favors clear skies (item 4 above). This effect is demonstrated in Figure 11, which shows zonal average and effective zonal reflectivities for a single day (January 1st). Here, we look at zonal properties as a convenient way of generating an ensemble of locations with the same solar geometry but differing cloud properties. Time averages at a specific location will behave similarly. Since the downward reflectivity has the downward shortwave at the top of the atmosphere in its denominator (equation 6), the zonal average and effective zonal downward reflectivities are the same (the gray line). The zonal mean upward reflectivity is very similar to the downward reflectivity but shows a difference due to solar geometry. The AM2 shortwave radiation is calculated with a two-stream technique that gives the diffuse radiation a mean inclination of 53^{o}. Consistent with this, the zonal average upward reflectivity is greater than the downward within a roughly 100^{o} wide band centered near the subsolar latitude at 23S. The effective zonal upward reflectivity is much smaller than the downward reflectivity and the zonal average upward reflectivity. This is because clear skies contribute disproportionately to the numerator and

denominator of equation 8 and have greater weight in the effective parameter. Stated another way, the average photon traveling up from the surface sees a clearer than average sky because clear skies supply more photons to the surface.

The weighting effect is critical to the accuracy of the 4-parameter method and is not properly represented in the three alternative techniques presented in the last section. This is the reason for the change in relationship between the ALL/CLR and 4-parameter upward reflectivities at different averaging lengths evident in Figure 8. If the ALL/CLR upward reflectivity were fit to the more accurate 4-parameter values, the fit would depend upon the relative frequency of clear and cloudy scenes in the time averaged fluxes. Hence the fit would be model dependent. Model dependent fitting is not practical because it requires instrumenting each model with extra shortwave calls to calibrate the fit. This instrumentation itself, with validation of albedo of zero, implements the 4-parameter technique.

In contrast to the case for the 4-parameter upward reflectivity, the weighting effect is not an important factor for the upward absorptivity. The zonal average upward absorptivity and the effective zonal upward absorptivity calculated from the daily data are very similar (not shown). As was noted in section 2, the clear and all sky upward absorptivities are more similar than are the clear and all sky values of the other atmospheric parameters. This reduces the impact of clear-cloud ensemble averaging on the upward absorptivity.

V. Conclusions and Discussion

A technique has been presented for characterizing the atmosphere's shortwave behavior with four parameters representing its bulk upward and downward properties. This model was shown to accurately predict the response of the surface and atmospheric budgets to changes in surface albedo. The zero-surface-albedo diagnostics used by the model are inexpensive to calculate and essential for accurate

characterization of the upward properties properties of the atmosphere. Three alternative techniques that do not have the benefit these diagnostics have reduced accuracy.

The albedos of a number of natural surfaces, including snow, have a strong spectral dependence in the shortwave band not represented in the AM2 model used here. Some other climate models do represent this by using several surface albedos for different shortwave sub-bands (e.g. Briegleb et al 2002). Since the radiation in the sub-bands is independent, this poses no difficulty for the technique presented here. In-situ shortwave diagnostics for the sub-bands may be used in combination with the zero surface albedo diagnostics to construct optical properties particular to each individual sub-band.

A simple application of the model is the calculation of the *maximum sea ice albedo feedback* (Covey et al 1991) – the radiative effect of globally replacing sea ice albedos with ocean albedos. Covey et al discuss the importance of this quantity, which is, in a sense, a counterpart to the cloud shortwave forcing. Covey et al made their calculation by making one-day sampling runs with the two surface albedos, ignoring the small cloud drift that occurred over this period. Having determined AM2's optical parameters, an accurate calculation can be made directly by using equation 11 with in situ albedos and with an alternative fixed ocean albedo of 0.1 in sea ice regions. Table 2 shows that, even for these models with surface conditions specified from observations, there are considerable differences in the maximum sea ice albedo feedback. These differences are mainly due to differences in atmospheric properties and demonstrate the potential for the atmospheric simulations to contribute to differences in the ice albedo feedback in a models. Hall (2004) makes use of a technique for evaluating a model's response to ice-albedo feedback -- temperature changes are compared for parallel 2 times CO_2 simulations with fixed and freely evolving surface albedos. Applying the 4-parameter technique to these experiments would allow the surface albedo forcing for the difference in temperature response to be calculated – effectively separating the surface albedo feedback from the other model feedbacks that impact the difference.

In principle, the 4-parameter technique could be applied to observations as well as models. It would be necessary to sample surface fluxes at several surface albedos to construct the parameters. This kind of sampling has been done using ship (Wendler 2004), aircraft (Freese and Kottmeier 1998), and fixed (Rouse 1987) observational platforms. Such observations are limited, however, and the combination of these measurements with TOA shortwave measurements by satellites, necessary to calculate all four parameters, raises the issue of scale. Ground based measurements alone would suffice to calculate the downward transmissivity and the upward reflectivity which, together, enable estimation of the surface absorption dependence upon surface albedo. If the weakness of the atmospheric compensation estimated with the GFDL model (Fig. 5) proves generally applicable, this would address the largest part of the surface albedo sensitivity problem.

The surface shortwave budget has also been estimated by combining satellite measurements with radiation models. The technique chosen by the WCRP for this purpose, the "Pinker" algorithm, generates zero surface albedo fluxes as a step in the algorithm (Whitlock et al 1995; Pinker and Laszlo 1992). Unfortunately, the zero surface albedo fluxes are not distributed with the data set. If they were, they would permit model optical properties to be compared with the effective optical properties used to calculate the "observed" surface fluxes, possibly lending insight into model and observational errors.

For models not yet instrumented with the extra diagnostics needed for the 4-parameter technique, the ALL/CLR method may prove a useful interim alternative. Although it is ad hoc, it has been shown to make reasonably accurate estimates of surface absorption at different albedos in the GFDL model. ALL/CLR does not provide as complete a description of the atmospheric optical properties as the 4-parameter technique. It estimates the upward reflectivity and, noting that $\tau_{\downarrow} = A_S(\alpha_S = 0)$, equation 19 gives the ALL/CLR estimate of atmospheric downward transmissivity as a special case. Since ALL/CLR does not estimate the upward absorptivity, it is restricted to the surface and cannot directly give the top of

atmosphere shortwave flux change due to a surface albedo change. Additionally, it does not make an estimate of the atmospheric downward reflectivity. To the extent that these extra diagnosed properties are useful for analysis of models, the 4-parameter technique has an additional advantage over the ALL/CLR method.

Acknowledgements

The author thanks Tony Beesley, V. Ramaswamy, Anthony DelGenio and two anonymous reviewers for helpful comments on this paper.

References

Briegleb, B.P., C.M. Bitz, E.C. Hunke, W.H. Lipscomb, and J.L. Schramm, 2002: *Description of the Community Climate System Model Version 2 Sea Ice Model*. National Center for Atmospheric Research, `http://www.ccsm.ucar.edu/csm/models/ccsm2.0/csim`.

Comiso, J.C., 2002: A rapidly declining perennial sea ice cover in the Arctic, *Geophys. Res. Lett.*, **29(20)**, p. 17(1-4).

Covey, C., K.E. Taylor, and R.E. Dickenson, 1991: Upper limit for sea ice albedo feedback contribution to global warming, *J. Geophys. Res.*, **96(D5)**, 9169—9174.

Freese, D. and Ch. Kottmeier, 1998: Radiation exchange between stratus clouds and polar marine surfaces, *Boundary-Layer Meteorology*, **87**, 331—356.

Freidenreich, S.M., and V. Ramaswamy, 1999: A new multiple-band solar radiative parameterization for general circulation models, *J. Geophys. Res.*, **104(D24)**, 31,389—31,409.

GFDL GAMDT, 2004: The new GFDL global atmosphere and land model AM2/LM2: Evaluation with prescribed SST simulations, *J. Climate*, **17(24)**, 4641--4673.

Hall, A., 2004: The role of surface albedo feedback in climate, *J. Climate*, **17**, 1550--1568.

Harrison, E.F, P. Minnis, B.R. Barkstrom and G.G. Gibson, 1993: Radiation budget at the top of the atmosphere *in* Atlas of Satellite Observations Related to Global Change, R.J. Gurney, J.L. Foster and C.L. Parkinson, eds., Cambridge University Press, 470pp.

Holland, M.M., and C.M. Bitz, 2003: Polar amplification of climate change in coupled models, *Climate Dynamics*, **21**, 221--232.

Kiehl, J.T., and K.E. Trenberth, 1997: Earth's annual global mean energy budget, *Bull. Amer. Met. Soc.*, **78(2)**, 197—208.

Pinker, R.T., and I. Laszlo, 1992: Modeling surface solar iradiance for satellite applications on a global scale, *J. Appl. Meteor.*, **31**, 194—211.

Rouse, W.R., 1987: Examples of enhanced global radiation through multiple reflection from an ice-covered Arctic sea, *Journal of Climate and Applied Meteorology*, **26**, 670—674.

Wang, X., and J.R. Key, 2003: Recent trends in Arctic surface, cloud, and radiation properties from space, *Science*, **299**, 1725—1728.

Wendler, G., B. Moore, B. Hartmann, M. Stuefer, and R. Flint, 2004: Effects of multiple reflection and albedo on the net radiation in the pack ice zones of Antarctica, *J. Geophys. Res.*, **109(D6)**, ???--???.

Whitlock, C.H., T.P. Charlock, W.F. Staylor, R.T. Pinker, I. Laszlo, A. Ohmura, H. Gilgen, T. Konzelman, R.C. DiPasquale, C.D. Moats, S.R. LeCroy and N.A. Ritchey, 1995: First global WCRP shortwave surface radiation budget data set, *Bull. Amer. Meteor. Soc.*, **76**, 1—18.

Table Captions

Table 1: Notation.

Table 2: Maximum sea ice albedo feedback, the impact on the global shortwave budget of replacing sea ice albedos with ocean albedos, for three atmospheric GCMs: CCM0, CCM1/BATS (Covey et al 1991), and AM2.

Figures Captions

Figure 1: The fraction of the downward shortwave at the surface that has been previously reflected from the surface (fractions less than 0.04 are not shaded) in the GFDL AM2 model.

Figure 2: The 4-parameter model

Figure 3: The AM2 annual climatological atmospheric optical parameters. The parameters are depicted schematically in Fig. 2 and based on equations 6—9. Note that $\varepsilon_{\uparrow} \equiv 1 - \alpha_{\uparrow} - \tau_{\uparrow}$ and $\varepsilon_{\downarrow} \equiv 1 - \alpha_{\downarrow} - \tau_{\downarrow}$.

Figure 4: Sensitivity of surface and atmospheric absorption to surface albedo as a fraction of the downward shortwave at the top of the atmosphere. These curves represent the annual climatological Arctic in AM2.

Figure 5: AM2's atmospheric compensation – the fractional reduction in surface albedo sensitivity of net shortwave flux at the top of the atmosphere from the sensitivity at the surface (see equation 14).

Figure 6: Monthly mean surface (left) and atmospheric (right) absorption at four validation albedos (0.2, 0.4, 0.6, and 0.8) plotted against the values estimated with the 4-parameter model. Every ninth grid point is plotted for clarity.

Figure 7: Linear (dashed black) and 2-parameter (dashed gray) and ALL/CLR (solid gray) approximations to the surface albedo dependent shortwave absorption. The 4-parameter estimates are also

shown (black). Actual absorptions from online radiation calculations at five validation albedos are also shown (circles). The 4-parameter technique is exact at zero surface albedo by construction.

Figure 8: 4-parameter upward reflectivity plotted against ALL/CLR upward reflectivity for daily (light marks) and monthly (dark marks) means.

Figure 9: RMS surface absorption error normalized by the local downward transmissivity for the four validation albedos (0.2, 0.4, 0.6, and 0.8) for all months and all locations on the globe (gray) and in the Arctic (black).

Figure 10: The difference in effective annual 4-parameter model downward and upward atmospheric reflectivities ($\alpha_{\downarrow} - \alpha_{\uparrow}$).

Figure 11: Daily downward and upward reflectivities: zonal average downward reflectivity (solid gray), zonal average upward reflectivity (solid black), and effective zonal upward reflectivity (dashed black).

Tables

Symbol	Definition
$S_{T\downarrow}$, $S_{T\uparrow}$	Downward and upward fluxes at the top of the atmosphere
$S_{B\downarrow}$, $S_{B\uparrow}$	Downward and upward fluxes at the surface
$\tau_{\downarrow}$, $\tau_{\uparrow}$	Atmospheric transmissivity to downward and upward shortwave
$\varepsilon_{\downarrow}$, $\varepsilon_{\uparrow}$	Atmospheric absorptivity to downward and upward shortwave
$\alpha_{\downarrow}$, $\alpha_{\uparrow}$	Atmospheric reflectivity to downward and upward shortwave
α_S	Surface reflectivity (albedo)
α_P	Planetary reflectivity (albedo)
A_S	Surface absorption ratio: $\left(S_{B\downarrow} - S_{B\uparrow}\right) / S_{T\downarrow}$
A_P	Planetary absorption ratio: $1-\alpha_P$
A_A	Atmospheric absorption ratio: A_P-A_S

Table 1: Notation.

Model	**Maximim Sea Ice Albedo Feedback (W/m^2)**
CCM0	3.0
CCM1/BATS	1.9
AM2	1.7

Table 2: Maximum sea ice albedo feedback, the impact on the global shortwave budget of replacing sea ice albedos with ocean albedos, for three atmospheric GCMs: CCM0, CCM1/BATS (Covey et al 1991), and AM2.

Figures

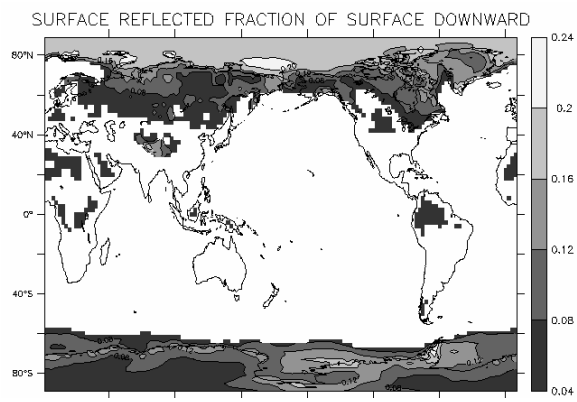

Figure 1: The fraction of the downward shortwave at the surface that has been previously reflected from the surface (fractions less than 0.04 are not shaded) in the GFDL AM2 model.

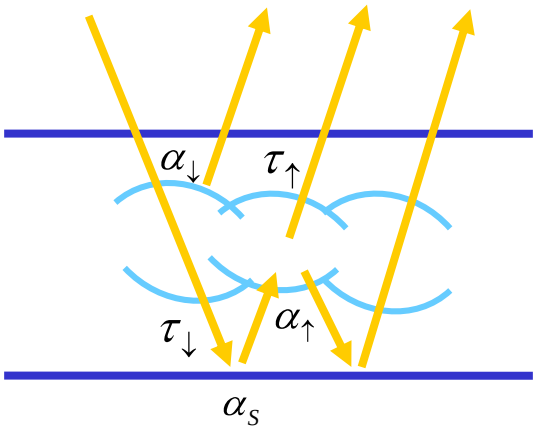

Figure 2: The 4-parameter model

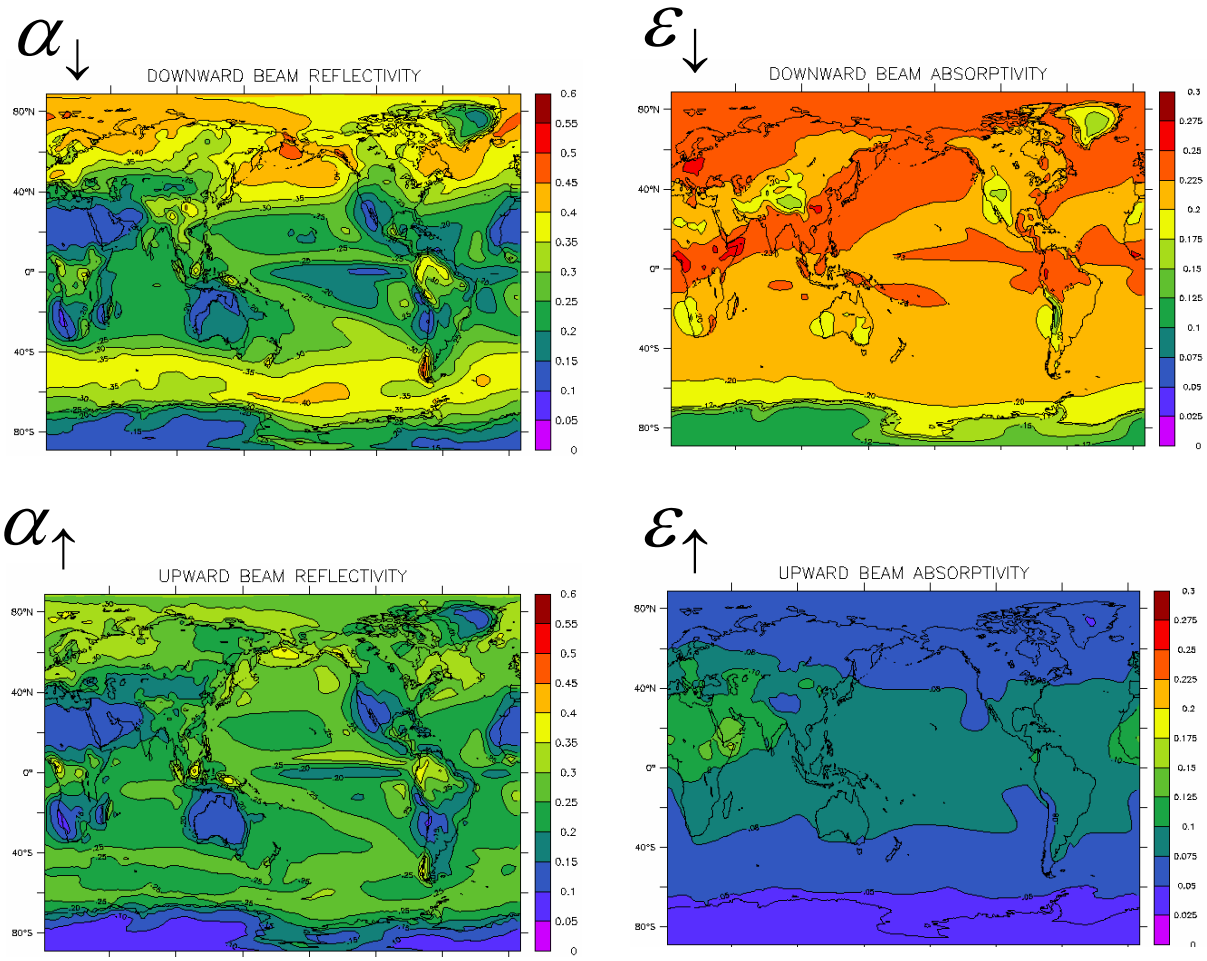

Figure 3: The AM2 annual climatological atmospheric optical parameters. The parameters are depicted schematically in Fig. 2 and based on equations 6—9. Note that $\varepsilon_{\uparrow} \equiv 1 - \alpha_{\uparrow} - \tau_{\uparrow}$ and $\varepsilon_{\downarrow} \equiv 1 - \alpha_{\downarrow} - \tau_{\downarrow}$.

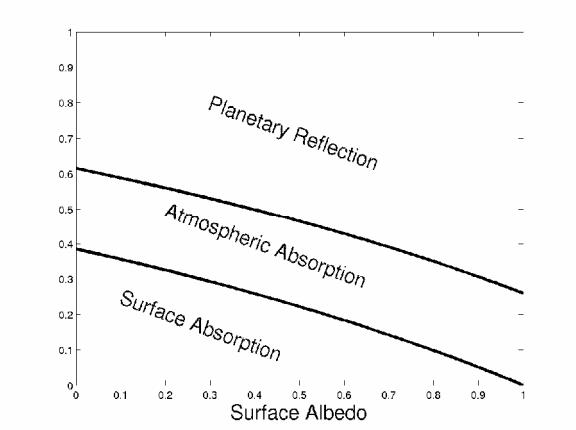

Figure 4: Sensitivity of surface and atmospheric absorption to surface albedo as a fraction of the downward shortwave at the top of the atmosphere. These curves represent the annual climatological Arctic in AM2.

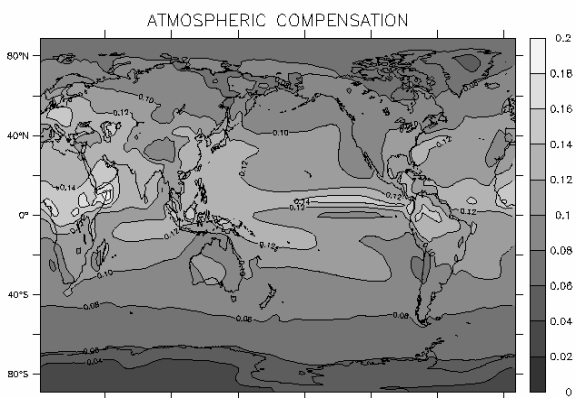

Figure 5: AM2's atmospheric compensation – the fractional reduction in surface albedo sensitivity of net shortwave flux at the top of the atmosphere from the sensitivity at the surface (see equation 14).

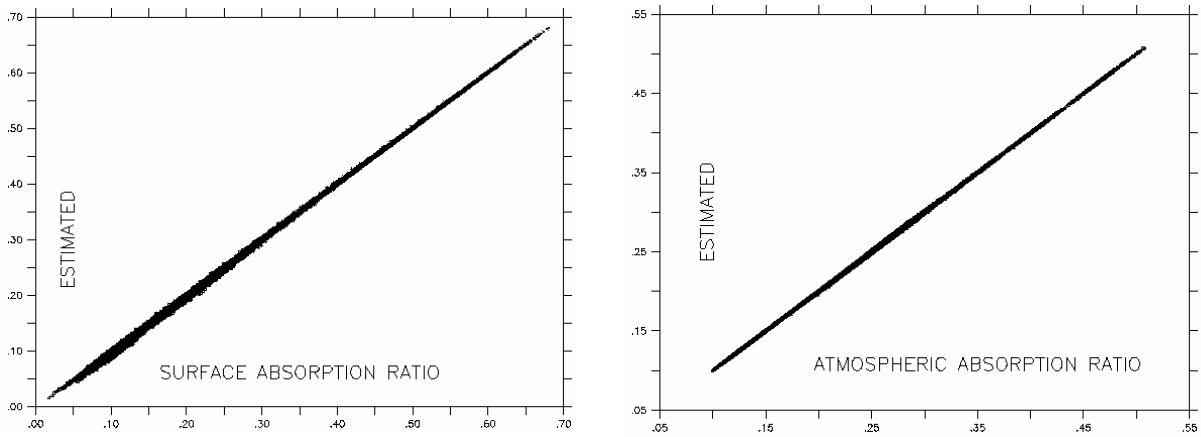

Figure 6: Monthly mean surface (left) and atmospheric (right) absorption at four validation albedos (0.2, 0.4, 0.6, and 0.8) plotted against the values estimated with the 4-parameter model. Every ninth grid point is plotted for clarity.

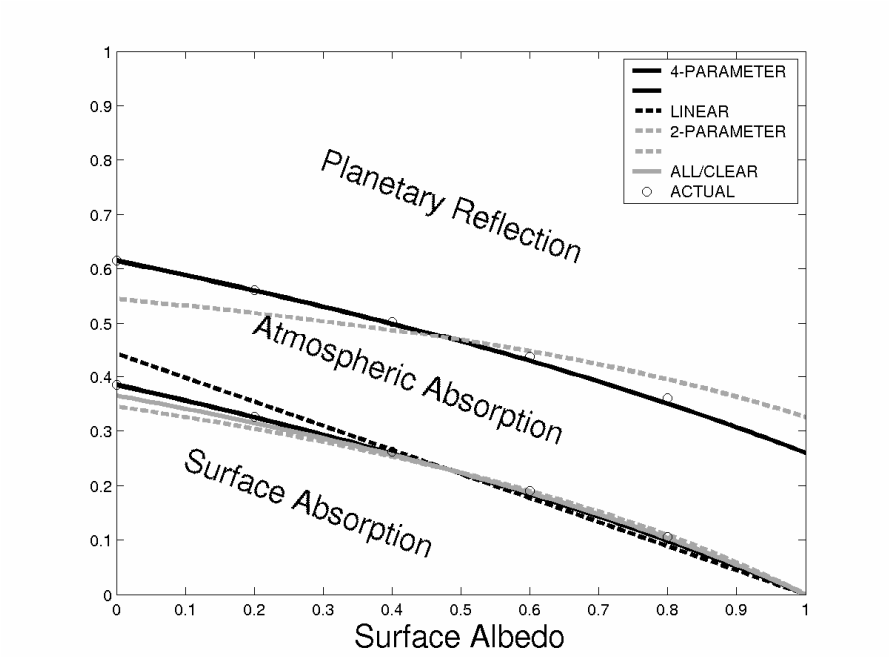

Figure 7: Linear (dashed black) and 2-parameter (dashed gray) and ALL/CLR (solid gray) approximations to the surface albedo dependent shortwave absorption. The 4-parameter estimates are also shown (black). Actual absorptions from online radiation calculations at five validation albedos are also shown (circles). The 4-parameter technique is exact at zero surface albedo by construction.

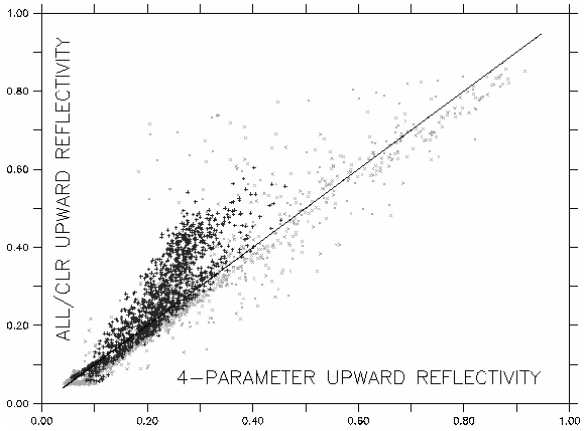

Figure 8: 4-parameter upward reflectivity plotted against ALL/CLR upward reflectivity for daily (light marks) and monthly (dark marks) means.

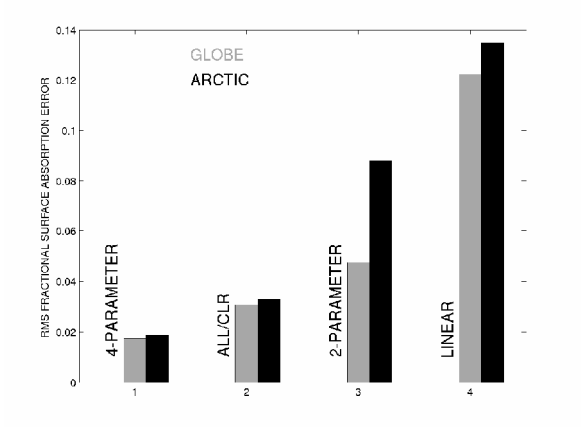

Figure 9: RMS surface absorption error normalized by the local downward transmissivity for the four validation albedos (0.2, 0.4, 0.6, and 0.8) for all months and all locations on the globe (gray) and in the Arctic (black).

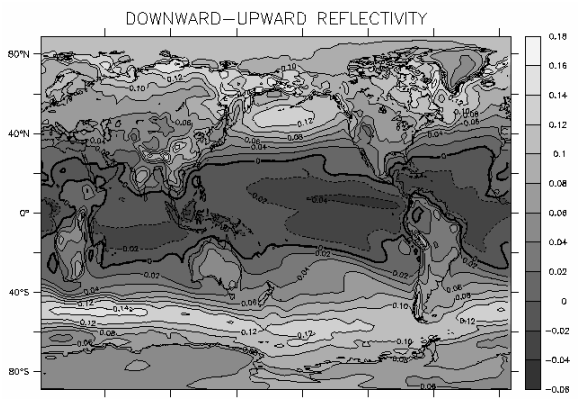

Figure 10: The difference in effective annual 4-parameter model downward and upward atmospheric reflectivities ($\alpha_{\downarrow} - \alpha_{\uparrow}$).

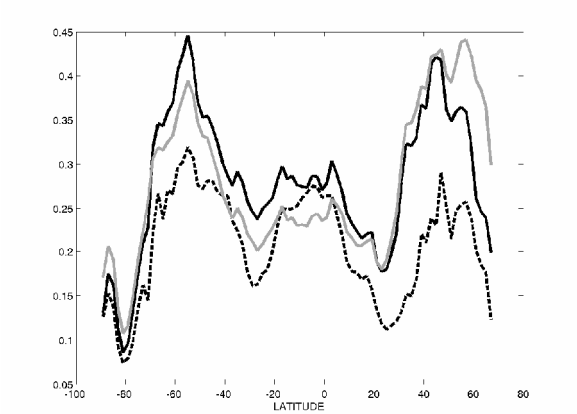

Figure 11: Daily downward and upward reflectivities: zonal average downward reflectivity (solid gray), zonal average upward reflectivity (solid black), and effective zonal upward reflectivity (dashed black).